



Diurnal variation in summer monsoon precipitation during active and break periods over central India and southern Himalayan foothills

Prasamsa Singh¹ and Kenji Nakamura¹

Received 7 July 2009; revised 14 January 2010; accepted 27 January 2010; published 26 June 2010.

[1] The diurnal variations of summer precipitation over central India and the southern Himalayan foothills are investigated using Tropical Rainfall Measuring Mission (TRMM) data for July–August from 1998 to 2007. The TRMM precipitation radar (PR) and Lightning Imaging Sensor (LIS) data are used to understand characteristics of precipitation. Daily data from TRMM/3B42 are used to determine active and break periods in central India on the basis of rainfall characteristics. Diurnal variation in rain rate, frequency of rain, conditional rain rate, storm height, and occurrence of convective rain is analyzed using TRMM/PR data ($0.1^\circ \times 0.1^\circ$ resolution). Diurnal variation in total lightning flashes is analyzed using TRMM/LIS data. The precipitation over central India during wet periods is characterized by a large amount of rainfall with a high frequency of rain and a secondary morning peak. The precipitation in dry periods is characterized by a strong diurnal variation with convective rainfall and enhanced electrical activity over central India. Characteristics of wet and dry periods over central India are generally supported over the southern Himalayan foothills.

Citation: Singh, P., and K. Nakamura (2010), Diurnal variation in summer monsoon precipitation during active and break periods over central India and southern Himalayan foothills, *J. Geophys. Res.*, 115, D12122, doi:10.1029/2009JD012794.

1. Introduction

[2] The summer monsoon of South Asia, which is a part of the Asian monsoon system, exhibits a wide spectrum of variability on diurnal, intraseasonal interannual, and decadal time scales [e.g., Yanai and Li, 1994; Yasunari, 1990; Krishnamurthy and Shukla, 2000]. The monsoon season possesses fluctuations of active periods and break periods caused by latitudinal oscillations of the monsoon trough. The basic characteristics of active and break periods have been studied extensively [e.g., Annamalai and Slingo, 2001; Gadgil and Joseph, 2003; Wang et al., 2005; Krishnan et al., 2000]. The active periods are generally associated with cyclonic vorticity and a decrease in surface pressure in the monsoon trough region extending from the head of the Bay of Bengal to a heat low over Pakistan along the Gangetic Plains. During the break periods, the monsoon trough shifts northward close to the Himalayan foothills and produces rain in those areas, but the rainfall decreases over northern and central parts of India [e.g., Ramamurthy, 1969; Desai and Mal, 1938; Krishnamurthy and Shukla, 2000].

[3] The characteristics of convective systems in active and break periods have been studied in monsoon-affected regions. For example, Rao et al. [2009], using mesosphere-

stratosphere-troposphere radar data over Gadanki, India (13.5°N , 79.2°E), observed more shallow convective systems in the dry spell than in wet spells.

[4] During the summer monsoon, thunderstorms with a single-cellular or a multicellular structure develop during the daytime over the land surface that is heated by solar radiation, forming clouds characterized by conditionally unstable thermodynamic stratification and weak vertical shear [Weisman and Klemp, 1982]. There are many previous studies showing that these kinds of thunderstorms usually develop in the summertime over landmasses [e.g., Kingsmill and Wakimoto, 1991; Shinoda and Uyeda, 2002; Shusse and Tsuboki, 2006; Case et al., 2008]. It is also plausible that soil moisture over the heated surface may significantly influence the evolution of air mass thunderstorms and the depth of the mixed boundary layer can influence the structure of the thunderstorms [McCaul and Cohen, 2002]. This depth may also control the amount of evaporation of the precipitating particles under the cloud base. Barnston and Schickedanz [1984] suggested that convective precipitation activity over the Great Plains increased because of modification of land use, such as irrigation. The impact of soil moisture on the potential of convection and the associated rainfall has been discussed using numerical models [e.g., Segal et al., 1995; Findell and Eltahir, 2003a, 2003b; Yamada, 2008].

[5] Diurnal variation of rainfall is one of the most important characteristics over a region governed by geophysical features and atmospheric dynamics that control

¹Hydrospheric Atmospheric Research Center, Nagoya University, Nagoya, Japan.

rainfall over the area. There have been numerous studies of the diurnal cycle of convection over South Asia [e.g., *Murakami*, 1983; *Ohsawa et al.*, 2001; *Fujinami et al.*, 2005; *Hirose and Nakamura*, 2005]. Over land, many areas exhibit an afternoon maximum of precipitation as expected from daytime heating; however, certain regions such as the Himalayan foothills and mountain basins have a late night and early morning maximum [e.g., *Barros et al.*, 2004; *Bhatt and Nakamura*, 2005]. The diurnal cycle of rainfall is usually dominated by the frequency of occurrence [*Dai et al.*, 2007]. Drizzle and nonshowery rainfall occur frequently in the morning over most land areas, whereas convective activity occurs in late afternoon [*Dai*, 2001]. *Nesbitt and Zipser* [2003] suggested that nocturnal rain in the tropics is often caused by mesoscale convective systems (MCSs), rather than isolated convection, and that MCSs are strongest after midnight, presumably because of the upscale growth of afternoon convection. *Yu et al.* [2007] indicated that the early morning peak mainly comes from long-duration rainfall events that last longer than 6 h, whereas the late afternoon peak mainly comes from rainfall events lasting less than 3 h. It was also observed that morning rainfall is enhanced over lakes in the Tibetan Plateau [*Singh and Nakamura*, 2009].

[6] The atmosphere in wet and dry spells is very different, and the precipitation systems could have different characteristics. The diurnal variation of the precipitation is one of the good indices characterizing precipitation systems. *Chakraborty and Krishnamurti* [2008] studied the diurnal variation of precipitation and cloudiness using different models during one active and one break period during the summer monsoon in 2000, but for limited periods. Thus, it is interesting to further investigate the diurnal variation of precipitation characteristics during wet and dry spells, which have not yet been well documented.

[7] The purpose of this study is to investigate diurnal variations in rainfall during wet and dry periods. The Tropical Rainfall Measuring Mission (TRMM) satellite was launched into a non-sun-synchronous orbit so that diurnal variation of precipitation can be studied [*Simpson et al.*, 1988]. Furthermore, the high vertical and spatial resolution of the TRMM precipitation radar (PR) permits three-dimensional studies even over complex terrain throughout the tropics. So, we used a TRMM data set for 10 years (1998–2007) with a grid size of $0.1^\circ \times 0.1^\circ$ latitude/longitude, selecting days of active periods and break periods during the Indian summer monsoon season (July–August). This paper is organized as follows: section 2 describes the data and methodology; results are presented in section 3; section 4 provides the discussion; and section 5 includes the summary and conclusions.

2. Data and Methodology

[8] For the study of diurnal variation of rainfall, TRMM data, GTOPO30 (Global 30 Arc Second Elevation data set), and National Centers for Environmental Prediction (NCEP) Reanalysis2 data were utilized.

2.1. TRMM

[9] For the study of diurnal variation of rainfall, TRMM PR 2A25 [*Iguchi et al.*, 2000] instantaneous data for 1998–

2007 were used. NASA and the Japan Aerospace Exploration Agency provided TRMM data products. We used level 2 precipitation radar data, version 6. Product 2A25 provided the near-surface rain rate from the PR. Algorithms for rain rate and rain types were described by *Iguchi et al.* [2000] and *Awaka* [1998], respectively. “Near surface” was defined as the lowest point in the clutter-free ranges in almost all cases. The near-surface height ranges from 500 m above ground level (AGL) at nadir to 2 km AGL at the swath edge. The average rain rate was calculated as a product of the conditional rain rate (near-surface rain rate more than 0 mm h^{-1}) and the frequency of rain (number of rain samples normalized by total number of samples). The mean rain rate is equivalent to accumulation of rain for certain periods. The PR 2A23 data provided “storm height.” Storm-height is the height of the storm top ($>18 \text{ dBZ}$). In this study, storm-height data were picked up only when rain was detected at the near surface using the PR 2A25 data set.

[10] The PR2A23 algorithm determines whether the echo is convective or stratiform based on the vertical profile of reflectivity (from which the bright-band, echo top height, and maximum reflectivity in the vertical profile are identified) and the horizontal variability of the echo. The PR convective-stratiform algorithm also assigns echo to a category called “other” when the echo is not classified as either convective or stratiform. Because of the small fraction of the other category and its very small contribution to total rain ($<0.2\%$ when using a 17 dBZ threshold), only convective and stratiform rain types were taken into consideration.

[11] To obtain climatological characteristics, gridded data were generated from the instantaneous data on a grid size of $0.1^\circ \times 0.1^\circ$ latitude/longitude for 3 h intervals. This grid size is almost double the PR pixel size (2×0.05).

[12] The TRMM 3B42 (version 6) daily rainfall data were used for selection of active and break periods. TRMM 3B42 data contain the estimated rain rate (mm h^{-1}) based on combination, passive microwave, and radar data from TRMM and infrared radiation data from the geostationary satellites [*Huffman et al.*, 1995, 1997, 2007]. The daily data of grid size $0.25^\circ \times 0.25^\circ$ were used for the period 1998–2007.

[13] The TRMM Lightning Imaging Sensor (LIS) space and domain data are utilized to analyze lightning flashes over the central India region. The data are available at <http://thunder.msfc.nasa.gov>. LIS is an optical sensor that uses a narrowband filter to detect lightning flashes and detects both intercloud and cloud-ground flashes. [*Christian et al.*, 1992].

2.1.1. Identification of Active and Break Periods

[14] Scientists have used different criteria and locations to define the active and break periods. Of the monsoon over India, many scientists [e.g., *Ramamurthy*, 1969; *Gadgil and Joseph*, 2003] have defined the break with positive anomalies of rainfall over the Himalayan foothills and southeastern peninsula. Some scientists [e.g., *Magana and Webster*, 1996; *Goswami and Ajayamohan*, 2001] defined breaks on the basis of the strength of the 850 hPa wind at a single grid point (15°N , 90°E). *Krishnan et al.* [2000] defined breaks as days with positive outgoing longwave radiation (OLR) anomalies over northwest and central India ($73^\circ\text{--}82^\circ\text{E}$, $18^\circ\text{--}28^\circ\text{N}$) exceeding 10 W/m^2 . *Annamalai and Slingo* [2001] used the daily all-India rainfall based on data at more than 200 stations representing the entire country. They defined the active

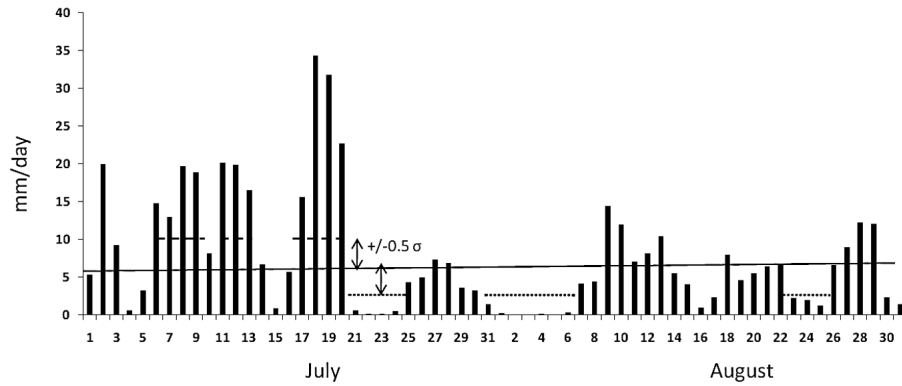


Figure 1. Daily data during July and August in 2000 over CIR. The process for selection of active days (dashed line) and break days (dotted line) is shown. The solid line shows the average for July–August. Active (break) phase is defined when daily rainfall is more (less) than 0.5σ from average.

phase when rainfall was $>20\%$ (>1 standard deviation) of the norm for a minimum of three consecutive days and the break phase when rainfall was $<20\%$ (<1 standard deviation) of the norm. *Rajeevan et al.* [2008] noted almost 80% of the active periods lasted 3–4 days over central India. *Ramamurthy* [1969] also noted that most of the breaks, in general, had a duration of about 3–5 days.

[15] This study used daily data from the 3B42 time series as an index of monsoon activity for 10 years during July and August. The active (break) phase is defined when daily rainfall over central India region (CIR, 73° – 78° E, 20° – 25° N) is more (less) than 0.5 standard deviation from the average of July–August for each year for a minimum of three consecutive days. For example, selection of active and break periods for 2000 is shown in Figure 1. On the basis of this

definition, composites of active-period rainfall and break-period rainfall were constructed. Figures 2 and 3 show composite maps of rain distribution for active and break periods, respectively. The CIR region was chosen by checking intra-seasonal variation of the rain distribution and is slightly different from others. We found 77 active days and 200 break days during July–August for 10 years (1998–2007). Although TRMM/PR have some sample error attributed to narrow swath, the results are significant. Figure 4 shows diurnal variation in rain rate (mm/h) for active days for the first half and last half of wet (active) periods over CIR. Even though two lines are not identical, they have two significant peaks. The composites of TRMM/PR data are consistent and agree well with other composites of active/break cycles created from different

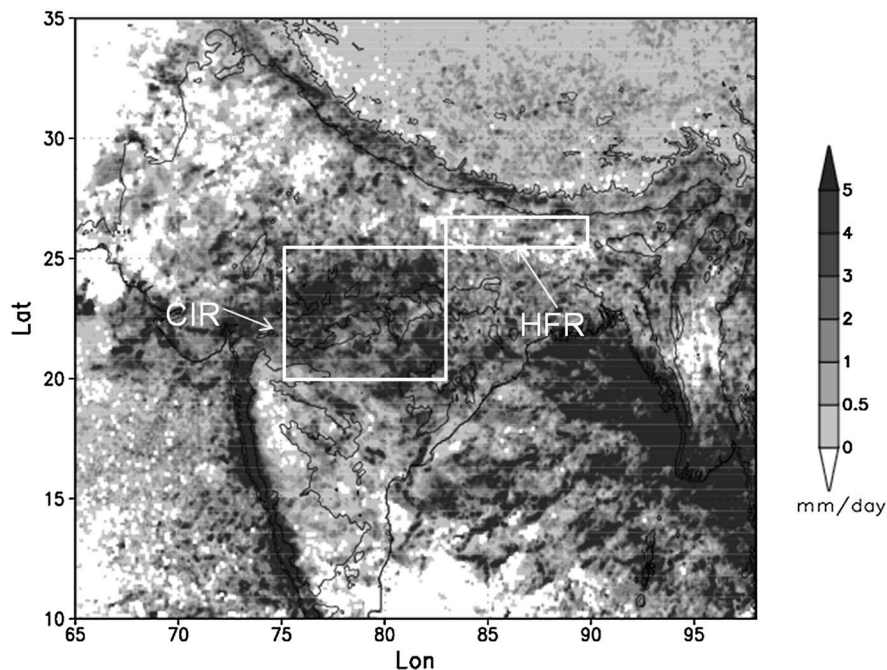


Figure 2. Composite map of rain distributions for active periods for 10 summers (July–August) from 1998 to 2007. Contour lines are for 500 and 2000 m surface elevation. CIR and HFR are study areas.

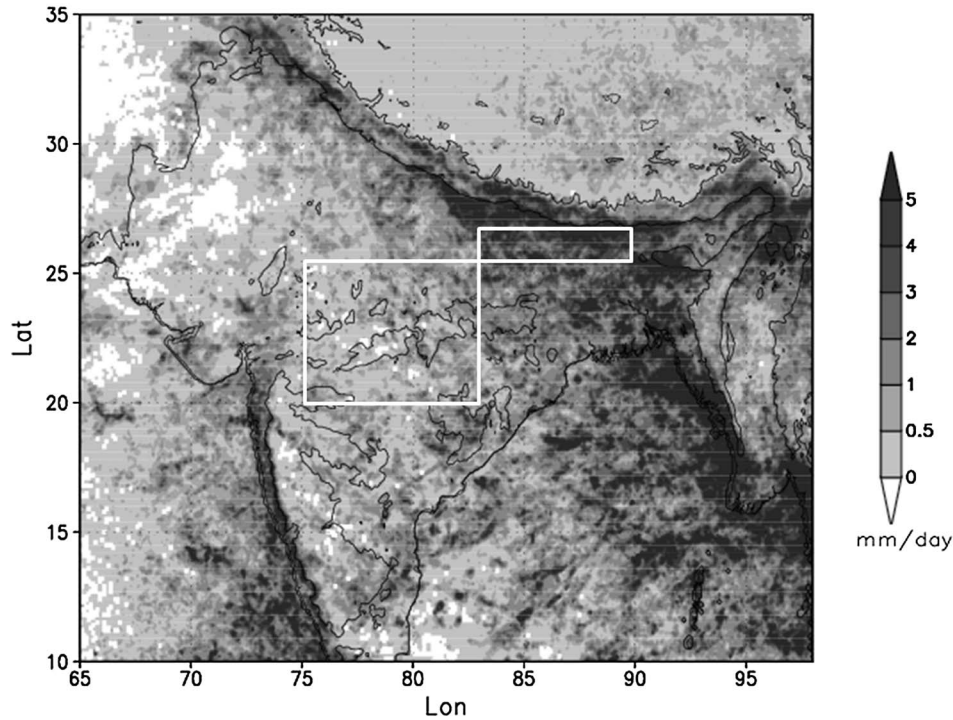


Figure 3. Composite map of rain distributions for break periods for 10 summers (July–August) from 1998 to 2007. Contour lines are for 500 and 2000 m surface elevation.

criteria [e.g., *Ramamurthy*, 1969; *Desai and Mal*, 1938]. The active and break days are similar to those mentioned by *Rajeevan et al.* [2008] with minimal differences. The longest break period (LBP) was observed in 2002, and the longest active periods (LAP) were observed in 2006.

[16] As the distribution of rain varies significantly between active and break periods, the absolute rain rate may not properly show characteristics of the diurnal variation. So, we have expressed the rain rate distribution in terms of rain fraction (RF) as

$$RF_h = \frac{R_h}{\sum_{h=1}^8 R_h} \quad (1)$$

where R is the rain rate and h is 3 hourly local time. This is a kind of normalized distribution and was also used for conditional rain rate and frequency of rain. In this study, the local time (LT) is time displacement from UTC, calculated from longitude.

[17] In the present study, 3 hourly rain rate totals were smoothed by using a 1:2:1 smoothing filter. The smoothed rain rate (SR) is given as

$$SR_h = \frac{R_{h-1} + 2R_h + R_{h+1}}{4}, \quad (2)$$

where R and h denote the rain rate and 3 hourly local time, respectively, as in the case of rain fraction computation. This smoothing was also used for conditional rain rate and frequency of rain, occurrence of convective rainfall, and total lightning flashes.

2.2. Other Data

[18] For the surface elevation, GTOPO30 data originally $0.008^\circ \times 0.008^\circ$ were modified to $0.1^\circ \times 0.1^\circ$ (available at [http://eros.usgs.gov/#/Find Data/Products and Data Available/gtopo30 info](http://eros.usgs.gov/#/Find+Data/Products+and+Data+Available/gtopo30+info)). For the surface temperature data, NCEP Reanalysis-2 data of $2.5^\circ \times 2.5^\circ$ latitude/longitude and the 6 hourly resolution data set (provided by NOAA and ESRL PSD, Boulder, Colorado; available at <http://www.cdc.noaa.gov>) were used. As 2002 has the longest break

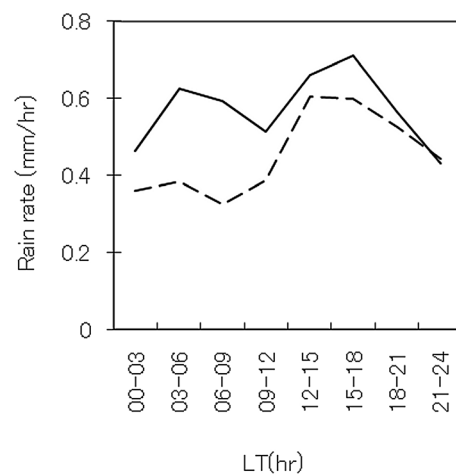


Figure 4. Diurnal variation in mean rain rate (mm/h) during wet periods for the first half (solid line) and the last half (dashed line) of wet periods over CIR.

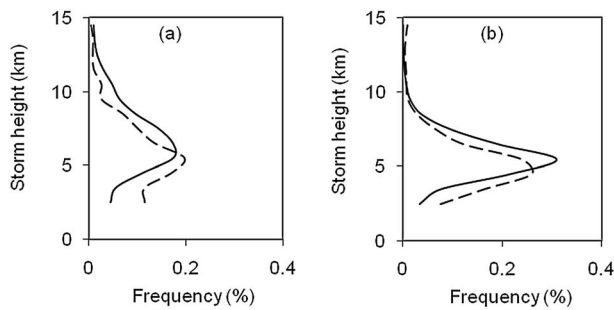


Figure 5. Frequency of storm height (%) during wet (solid line) and dry (dashed line) periods for (a) convective rain and (b) stratiform rain for over CIR.

periods (27 days) and 2006 has the longest active periods (14 days) within the period 1998–2007, surface temperature was studied for the LBP in 2002 and the LAP in 2006 over CIR.

3. Results

3.1. General Characteristics of Precipitation During Active and Break Periods

[19] Here we describe characteristics of active and break periods in July and August over central India and the southern flank of the southern Himalayan region.

[20] During the active periods, rainfall is concentrated over the central region and decreases over the Himalayan foothill region (Figure 2). In contrast, during break periods, rainfall decreases over the central India region and increases over the southern Himalayan foothill region, especially over the eastern part (Figure 3). Other regions also show some distinct characteristics, for example, the rain amount along the West Ghats mountain range and over the Bay of Bengal is greater for active periods. These characteristics are similar to findings of other researchers [e.g., Ramamurthy, 1969; Desai and Mal, 1938; Krishnamurthy and Shukla, 2000; Rajeevan *et al.*, 2008].

[21] To study rainfall characteristics in detail during wet periods (active periods over central India and break periods over the Himalayan foothills) and dry periods (break periods over central India and active periods over the southern Himalayan foothills), study areas CIR and the Himalayan foothill region (HFR) are selected (Figure 2). During wet periods (dry periods), CIR receives rainfall of about 4.1 mm/d (0.7 mm/d), and HFR receives about 3.64 mm/d (0.97 mm/d) (data not shown).

[22] Figures 5a and 5b depict the vertical profile of frequency of storm height from 1 to 15 km during wet and dry periods for stratiform and convective rain, respectively. Convective rain appeared more frequently during dry periods than during wet periods, with a sharp peak around 5 km but stratiform rain appeared more frequently during wet periods than during dry periods, with a broad peak above 5 km. However, storm height is higher during wet periods for both types of rain. The stratiform rain has a radar bright band just below the freezing level where the radar echo is enhanced. This enhancement could cause a high probability of the storm height at the 0°C isotherm level, which is around 4–5 km

in summer. A greater frequency of shallow systems in dry periods may be due to many shallow systems categorized as convective. It is well known that the storm height distribution is bimodal over the ocean, where much shallow convection exists [Short and Nakamura, 2000]. However, Figure 5 shows that over CIR, the storm height is mono-dispersed, and shallow systems are relatively more frequent in the dry periods. This fact may mean that the shallow convection over CIR is different from those over oceans controlled by the trade wind inversion.

3.2. Diurnal Variation in Active and Break Periods

[23] Here we will describe details of diurnal variation during wet and dry periods over CIR and HFR.

[24] Figure 6a shows 3 hourly unconditional rain rate distributions for wet and dry periods over CIR. During wet periods, the rain rate is greater than 0.4 mm h^{-1} , whereas during dry periods, the rain rate is less than 0.2 mm h^{-1} . To see the strength of the diurnal variation in rain, rain is expressed in rain fraction (Figure 6b). During wet periods, the rain rate shows a weak diurnal variation with a broad peak in the afternoon around 15 LT. During dry periods, the rain rate shows a strong diurnal variation with a narrow peak at around 15 LT. Figure 6c shows 3 hourly fractions of frequency of rain for wet and dry periods over CIR. During wet periods, broad peaks of frequency of rainfall centered at night (18–21 LT) and morning (03–06 LT) appear. During dry periods, a peak is observed in the afternoon around 15 LT. Figure 6d shows the diurnal variation in conditional rain rate for wet and dry periods expressed as a fraction. During wet periods, two broad peaks are observed in the afternoon (12–18 LT) and around early morning (03–06 LT), but for dry periods, a sharper peak is observed in the afternoon (12–18 LT). The amplitude of the diurnal variation of frequency of rain is stronger for the dry periods but is not as strong as the conditional rain rate. Figure 6 implies that the conditional rain rate contributes much to the intensity of the diurnal variation in dry periods, which agrees with data from Nesbitt and Zipser [2003] but contradicts the results of Dai *et al.* [2007]. During wet periods, peaks for frequency of rain and conditional rain rate occur in the afternoon. Frequency of rain lags conditional rain rate by a few hours. Figure 7 shows the occurrence of convective rain (number of convective rain pixels divided by that of rain pixels) for wet and dry periods. Similar to Schumacher and Hauxe [2003], the two lines are very similar with peaks at 12 LT, but with a difference of about 10%. During wet periods, occurrence of convective rain is less than 20%, but during dry periods, more than 18% is seen throughout the day. Compared to Figure 6a, the peak in the dry periods and that in the afternoon in the wet periods seems to be associated with convective rain, but the early morning peak in the wet periods does not seem to be associated with convective rain.

[25] Figure 8a shows the 3 hourly total numbers of lightning flashes for wet and dry periods. The total number of flashes in wet periods is much more than in dry periods, but the peak time is around the same time, 15–18 LT. The peak local time in wet and dry periods is delayed by a few hours. To see the total number flashes with relation to rain, the total number of flashes is normalized by frequency of rain at each 3 hourly slot (Figure 8b). The flashes normalized by frequency of rain in break periods are clearly higher

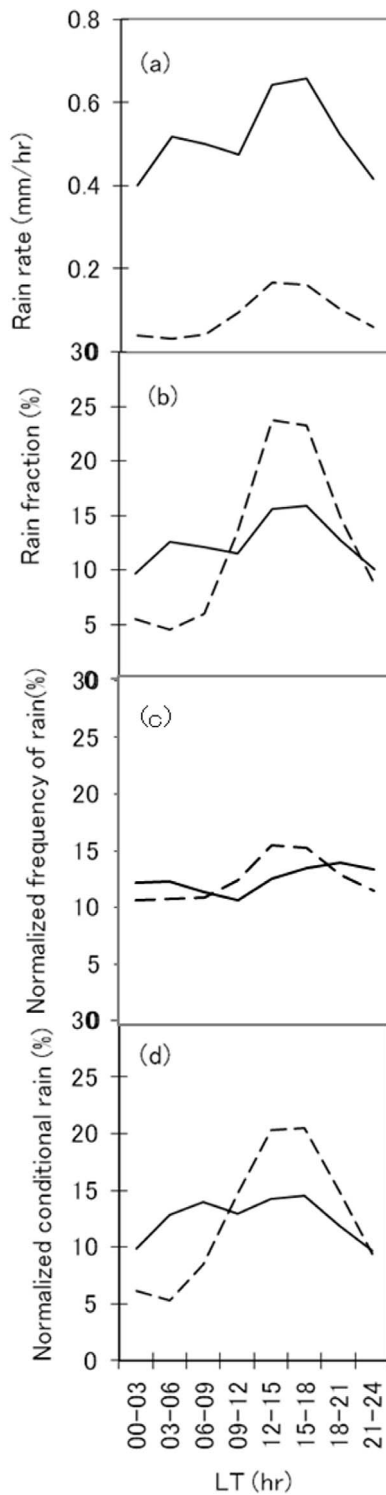


Figure 6. Diurnal variation during wet (solid line) and dry (dashed line) periods for (a) mean rain rate (mm/h), (b) rain fraction (%), (c) normalized frequency of rain (%), and (d) normalized conditional rain (%) over CIR.

than in active periods. During dry periods, a peak of flashes normalized by frequency of rain is observed at 18–21 LT, and a dip is observed at 06–09 LT. During wet periods, the peak is observed at 15–18 LT, and a dip is observed

at 00–03 LT. Flashes normalized by frequency of rain at the peak in dry periods are twice as large as during wet periods, which can be interpreted as dry periods having twice as many flashes for the same frequency of rain as wet periods. Figure 8c is the same as Figure 8b but normalized by the mean rain rate at each 3 hourly time slot. The flashes are about 6 times more in dry periods for the same rain amount. The broad dip in dry periods appears to be a combination of low rain rates during midmorning. Williams *et al.* [1992] noted the significant lightning over the Darwin region during dry periods. Zipser [1994] and Takayabu [2006] observed rain yield (the amount of rain divided by the frequency of flashes) is lowest where most intense convective activity is observed.

[26] Overall, the average storm height is higher during wet periods than during dry periods, but the difference is small (data not shown). The lowering of the storm height in the dry periods may be due to the greater number of shallow convective storms suggested in Figure 5a. Figure 9 shows the 6 hourly diurnal variations in near-surface temperature (1000 hPa) from NCEP data for LAP and LBP over CIR. The peak of the temperature is observed at 12–18 LT for both active and break periods with about 30°C and 34°C, respectively. The temperature is almost constant throughout the day during wet periods, but during dry periods, there is about 7°C difference throughout the day. This fact may simply be due to the difference of clouds and the soil moisture. Rao [1986] observed that the sensible heat flux is generally larger during the dry monsoon than in the wet monsoon. Many researchers have seen positive anomalies of OLR during break periods and negative anomalies of OLR during active periods [e.g., Krishnan *et al.*, 2000; Gadgil and Joseph, 2003] over CIR. These observations also support higher surface temperature and less cloud during dry periods than in wet periods. Thus, afternoon convective rainfall during dry periods is thought to be caused by strong solar heating.

[27] Figure 10a shows the diurnal cycle in the 3 hourly rain rate over HFR. The rain rate is more than 0.3 mm h⁻¹

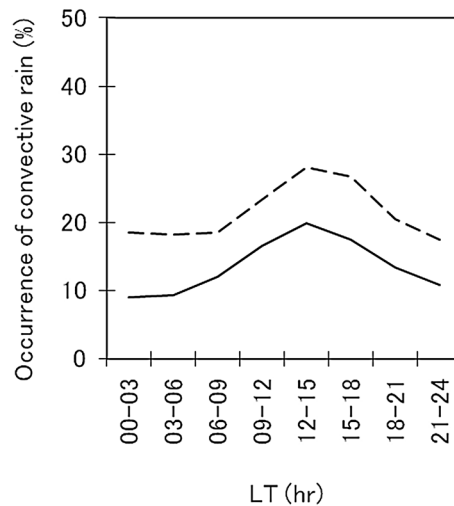


Figure 7. Diurnal variation of occurrence of convective rain during wet (solid line) and dry (dashed line) periods over CIR.

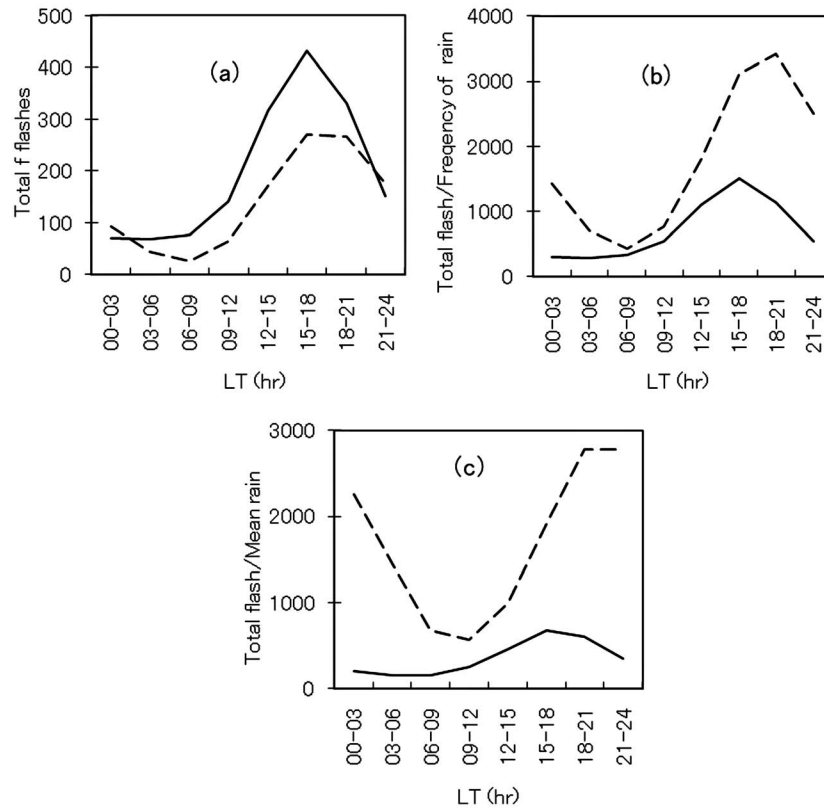


Figure 8. Diurnal variation during wet (solid line) and dry (dashed line) periods for (a) total number of lightning flashes during, (b) normalized total number of flashes by frequency of rain, and (c) normalized total by mean rain rate over CIR.

during wet periods, whereas it is less than 0.2 mm h^{-1} during dry periods. To compare the diurnal variation more easily, the rain rate is expressed as a rain fraction (Figure 10b). During wet periods, a stronger diurnal variation appears with a peak at around morning (03–09 LT), and during dry periods, the peak is around 09–12 LT. The morning enhancement also appears over CIR (Figure 6), but over HFR, the enhancement is much stronger and with only one peak in the diurnal variation. The peak local time in rain for the dry periods of about 09–12 LT is a few hours ahead of that over CIR. Figure 10c shows the diurnal variation in normalized rain frequency over HFR for dry and wet periods. Both patterns of diurnal variation have peaks in early morning. During wet periods, a peak appears around 06–09 LT, and during dry periods, a peak is seen at around 03–06 LT. Figure 10d shows the diurnal variation in normalized conditional rain rate. Compared to Figure 10c, the amplitude of the diurnal variation in both rain frequency and conditional rain rate in each period is almost the same; that is, the dip-to-peak percentages are 13–16% and 9–17% for dry periods and 9–17% and 10–15% for wet periods. For dry periods, both peaks appear in the morning but with a phase shift; that is, the peak appears at 03–06 LT in the frequency and 09–12 LT in the conditional rain rate. For wet periods, the conditional rain rate has a peak in the early morning, and the frequency is slightly delayed. Compared to Figure 10b, Figure 10d shows a similar pattern to the rain fraction, and in both, the peak

appears slightly greater during the wet periods than in dry periods. Figure 11 shows the occurrence of convective rain over HFR. Strong diurnal variation appears during wet periods with a peak around 15–18 LT, while during wet periods, weak diurnal variation is shown with a peak at 12–15 LT.

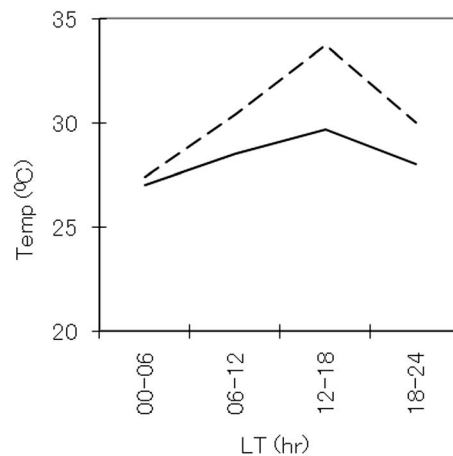


Figure 9. Diurnal variation in near-surface temperature (1000 hPa) during LAP (solid line) and LBP (dashed line) over CIR.

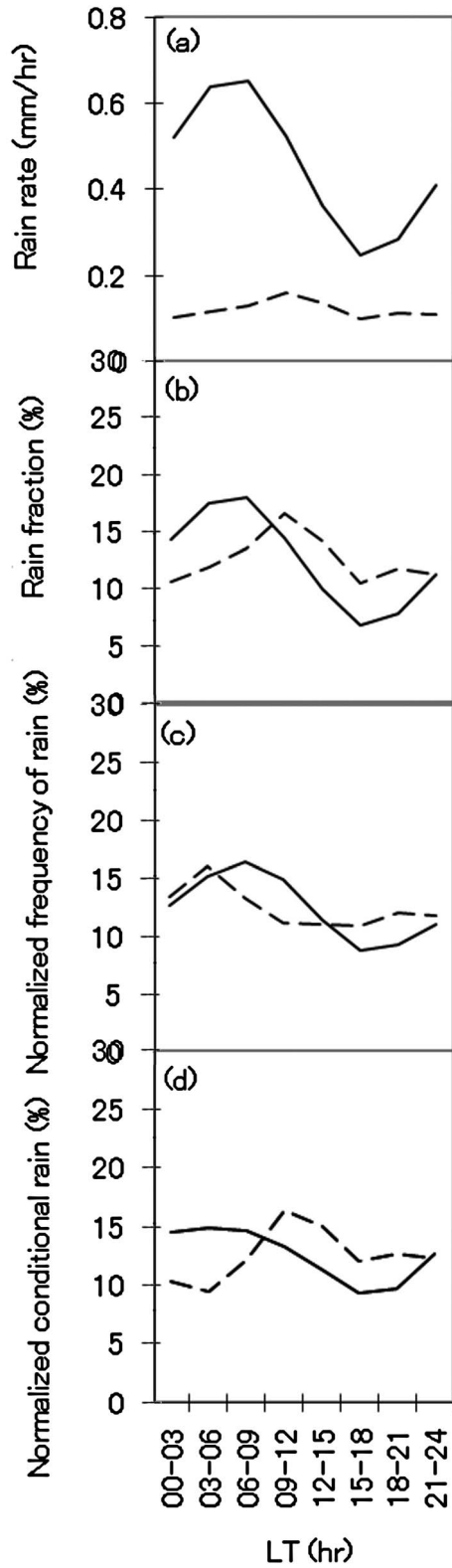


Figure 10. Diurnal variation during wet (solid line) and dry (dashed line) periods in (a) rain rate (mm/h), (b) rain fraction (%), (c) normalized frequency of rain (%), and (d) normalized conditional rain (%) over HFR.

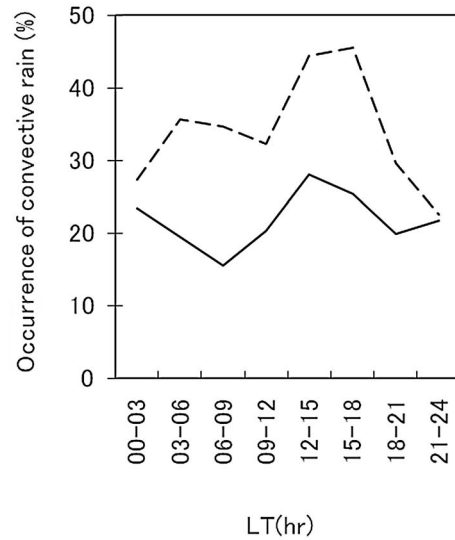


Figure 11. Diurnal variation in occurrence of convective rain during wet (solid line) and dry (dashed line) periods over HFR.

During wet periods, storm height is higher than dry periods by nearly 1 km over HFR (data not shown).

4. Discussion

[28] CIR does not have major mountain ranges, and the topographical forcing may be small. Thus, the characteristics of the diurnal variation could be more uniform over the CIR. In dry periods, the diurnal variation in the rain fraction is strong (Figure 6b). The diurnal variation in frequency of rain and conditional rain rate is also strong (Figures 6c and 6d). Since the mean rain rate is the product of conditional rain rate and rain frequency, both rain frequency and conditional rain rate contribute to the diurnal variation of rain amount. However, the diurnal variation of conditional rain rate is much stronger than that of rain frequency. This means that conditional rain rate mainly contributes to rain amount. For wet periods, the diurnal variation is small, and a phase difference exists between rain frequency and conditional rain rate. The phase difference means that the diurnal growth of rain amount to its peak is first affected by conditional rain rate, followed by rain frequency. In addition, morning rain enhancement exists. Lightning shows the characteristics more clearly; that is, in dry periods, lightning more frequently occurs than in wet periods for the same amount of rain. The peak time is at 18–21 LT, which is delayed from the rain amount, etc., by a few hours but precedes that of storm height. The fraction of convective rain also supports that the precipitation systems are convective in break periods. Precipitation systems in wet periods seem temporally more stable and “quiet” than those in dry periods. In other words, the systems in wet periods exist in a nearly saturated environment. On the other hand, the systems in dry periods exist in an unsaturated environment and could develop quickly and once convective inhibition is overcome by the effects of daytime heating.

[29] Since lightning occurs in strong turbulent conditions with solid-phase particles, the high flash rate in dry periods means strong updrafts with deep convection. This also supports that the precipitation in dry periods occurs with stronger convection. The time delay in peak flash rate and the storm height (data not shown) in dry periods from the rain amount, conditional rain rate, and rain frequency is a puzzle. The peak time coincidence of rain amount, rain frequency, and conditional rain rate may mean that the precipitation system develops in a short time, but they are not associated with lightning or high storm height.

[30] The results for HFR seem more complicated. The morning rain is dominant or, at least, plays a major role. The morning rain is thought to be due to mountain/valley winds originating from the Himalayan southern slopes. For dry periods, frequency of rain and conditional rain rate have different peak times. Peak time of the rain rate is very similar to the conditional rain rate. The variations in wet periods are nearly coherent in rain amount, rain frequency, and conditional rain rate with clear morning peaks. This fact suggests that in wet periods, the precipitation systems are strongly controlled by the Himalayan slope. During dry periods, a peak in rain amount and conditional rain rate appear around 09–12 LT. Morning rain and afternoon-evening rain are easy to understand; however, the peak in late morning is difficult to understand. This might be because of the limited number of samples. The peaks in frequency of rain and occurrence of convective rain are around 03–06 LT and 15–18 LT. These peaks could be understood as follows: the morning peak is due to the Himalayan slope, and the afternoon peak is due to solar radiation. Our analyses are only for CIR and HFR. It is of interest to see the diurnal characteristics over other regions. Rafiuddin et al. [2009] analyzed premonsoon and monsoon precipitation systems around Bangladesh. They suggested that in the mature monsoon season, the precipitation systems are many, but small. The summer atmosphere around Bangladesh must be very humid, and the precipitation systems are shallow. This fact suggests that the precipitation systems may first be categorized by the abundance of moisture in the lower troposphere. We need more rigorous investigation using models to confirm the suggestion.

5. Summary and Conclusion

[31] The summer monsoon season possesses fluctuations of active periods and break periods caused by latitudinal oscillations of the monsoon trough. This study used daily data from the 3B42 time series as an index of monsoon activity for 10 years during July and August. The active and break periods are defined by the daily rainfall over CIR. During the period, we found 77 active days and 200 break days. Composite maps show increased rainfall over the Himalayan region and over the southeastern peninsula of India when rainfall decreases over central India during break periods, and vice versa during active periods.

[32] During wet periods over CIR, the major diurnal peak of rain is observed at 12–18 LT, similar to dry periods, but a minor peak appears at 03–06 LT. HFR receives higher amounts of rainfall with strong diurnal variation during wet periods than during dry periods. During wet periods, a broad peak is observed in the morning (03–09 LT), but during dry

periods, a peak is observed during late morning (09–12 LT) over HPR.

[33] Over CIR, the diurnal variation in conditional rain rate and occurrence of convective rainfall is stronger during dry periods than during wet periods. Total flash per frequency of rain and total flash per mean rain rate are also higher during dry periods than during wet periods. However, storm height is lower during dry periods than during wet periods.

[34] Over HFR, more afternoon convective rainfall appears during dry periods than during wet periods, but storm height is lower during dry periods than during wet periods. These characteristics are similar to the characteristics over CIR during dry periods.

[35] Furthermore, characteristics of diurnal variation of dry and wet periods will be studied using models.

[36] **Acknowledgments.** We thank T. Yasunari (Nagoya University) and D. Short (National Institute of Information and Communications) for many valuable discussions and for help in polishing this manuscript. We are grateful to E. J. Zipsper and two anonymous reviewers for comments and suggestions that led to significant improvements in this manuscript. The TRMM data were provided by JAXA. The study was supported by JAXA through the TRMM project.

References

- Annamalai, H., and J. M. Slingo (2001), Active/break cycles: Diagnosis of the intraseasonal variability of the Asian summer monsoon, *Clim. Dyn.*, *18*, 85–102, doi:10.1007/s003820100161.
- Awaka, J. (1998), Algorithm 2A23-Rain type classification, paper presented at Symposium on the Precipitation Observation from Non-Sun Synchronous Orbit, ESTO, Nagoya, Japan.
- Barnston, A. G., and P. T. Schikedanz (1984), The effect of irrigation on warm season precipitation in the southern Great Plains, *J. Clim. Appl. Meteorol.*, *23*, 865888, doi: 10.1175/1520-0450(1984)023<0865:TEOIOW>2.0.CO;2.
- Barros, A. P., G. Kim, E. Williams, and S. W. Nesbitt (2004), Probing orographic controls in the Himalayas during the monsoon using satellite imagery, *Nat. Hazards Earth Syst. Sci.*, *4*, 29–51.
- Bhatt, B. C., and K. Nakamura (2005), Characteristics of monsoon rainfall around the Himalayas revealed by TRMM precipitation radar, *Mon. Weather Rev.*, *133*, 149–165, doi:10.1175/MWR-2846.1doi:10.1175/MWR-2846.1.
- Case, J. L., W. L. Crosson, S. V. Kumar, W. M. Lapenta, and C. D. Peters-Lidard (2008), Impacts of high-resolution land surface initialization on regional sensible weather forecast from the WRF model, *J. Hydrometeorol.*, *9*, 1249–1266, doi:10.1175/2008JHM990.1.
- Chakraborty, A., and T. N. Krishnamurti (2008), Improved forecasts of the diurnal cycle in the tropics using multiple global models. Part II: Asian summer monsoon, *J. Clim.*, *21*, 4045–4067, doi:10.1175/2008JCL12107.1.
- Christian, H. J., R. J. Blakeslee, and S. J. Goodman (1992), Lightning Imaging Sensor (LIS) for the Earth Observing System, NASA Tech. Memo., TM-4350.
- Dai, A. (2001), Global precipitation and thunderstorm frequencies. Part II: Diurnal variations, *J. Clim.*, *14*, 1112–1128, doi:10.1175/1520-0442(2001)014<1112:GPATFP>2.0.CO;2.
- Dai, A., X. Lin, and K. Hsu (2007), The frequency, intensity, and diurnal cycle of rainfall in surface and satellite observations over low- and mid-latitudes, *Clim. Dyn.*, *29*, 727–744, doi:10.1007/s00382-007-0260-y.
- Desai, B. N., and S. Mal (1938), Thunder squalls of Bengal, *Beiter Geophys.*, *52*, 285–304.
- Findell, K. L., and E. A. B. Eltahir (2003a), Atmospheric controls on soil moisture-boundary layer interactions. Part I: Framework development, *J. Hydrometeorol.*, *4*, 552–569, doi:10.1175/1525-7541(2003)004<0552:ACOSML>2.0.CO;2.
- Findell, K. L., and E. A. B. Eltahir (2003b), Atmospheric controls on soil moisture-boundary layer interactions. Part II: Feedbacks within the continental United States, *J. Hydrometeorol.*, *4*, 570–583, doi:10.1175/1525-7541(2003)004<0570:ACOSML>2.0.CO;2.
- Fujinami, H., S. Nomura, and T. Yasunari (2005), Characteristics of diurnal variations in convection and precipitation over the southern Tibetan

- Plateau during summer, *SOLA*, 1, 49–52, doi:10.2151/sola.2005-014doi:10.2151/sola.2005-014.
- Gadgil, S., and P. V. Joseph (2003), On breaks of the Indian monsoon, *Proc. Indian Acad. Sci.*, 112, 529–558.
- Goswami, B. N., and R. S. Ajayamohan (2001), Intraseasonal oscillations and interannual variability of the Indian summer monsoon, *J. Clim.*, 14, 1180–1198, doi:10.1175/1520-0442(2001)014<1180:IOAIVO>2.0.CO;2.
- Hirose, M., and K. Nakamura (2005), Spatial and diurnal variation of precipitation systems over Asia observed by the TRMM precipitation radar, *J. Geophys. Res.*, 110, D05106, doi:10.1029/2004JD004815.
- Huffman, G. J., R. F. Adler, B. Rudolf, U. Schneider, and P. R. Keehn (1995), Global precipitation estimates based on a technique for combining satellite-based estimates, rain gauge analysis, and NWP model precipitation information, *J. Clim.*, 8, 1284–1295, doi:10.1175/1520-0442(1995)008<1284:GPEBOA>2.0.CO;2.
- Huffman, G. J., R. F. Adler, P. Arkin, A. Chang, R. Ferraro, A. Gruber, J. Janowiak, A. McNab, B. Rudolph, and U. Schneider (1997), The Global Precipitation Climatology Project (GPCP) combined precipitation dataset, *Bull. Am. Meteorol. Soc.*, 78, 5–20, doi:10.1175/1520-0477(1997)078<0005:TGPCPG>2.0.CO;2.
- Huffman, G. J., R. F. Adler, D. T. Bolvin, B. Gu, E. J. Nelkin, K. P. Bowman, Y. Hong, E. F. Stocker, and D. B. Wolff (2007), The TRMM multi-satellite precipitation analysis: Quasi-global, multi-year, combined-sensor precipitation estimates at fine scales, *J. Hydrometeorol.*, 8, 38–55, doi:10.1175/JHM560.1.
- Iguchi, T., T. Kozu, R. Meneghini, J. Awaka, and K. Okamoto (2001), Rain-profiling algorithm for the TRMM precipitation radar, *J. Appl. Meteorol.*, 39, 2038–2052, doi:10.1175/1520-0450(2001)040<2038:RPAFTT>2.0.CO;2.
- Kingsmill, D. E., and R. M. Wakimoto (1991), Kinematic, dynamic, and thermodynamic analysis of a weakly sheared severe thunderstorm over northern Alabama, *Mon. Weather Rev.*, 119, 262–297, doi:10.1175/1520-0493(1991)119<0262:KDATAO>2.0.CO;2.
- Krishnamurthy, V., and J. Shukla (2000), Intra-seasonal and inter-annual variations of rainfall over India, *J. Clim.*, 13, 4366–4375, doi:10.1175/1520-0442(2000)013<0001:IAIVOR>2.0.CO;2.
- Krishnan, R., C. Zhang, and M. Sugi (2000), Dynamics of breaks in the Indian summer monsoon, *J. Atmos. Sci.*, 57, 1354–1372, doi:10.1175/1520-0469(2000)057<1354:DOBITI>2.0.CO;2.
- Magana, V., and P. J. Webster (1996), Atmospheric circulations during active and break periods of the Asian monsoon, paper presented at Eighth Conference on Global Ocean–Atmosphere–Land System (GOALS), Am. Meteorol. Soc., Atlanta, Ga.
- McCaul, E. W., Jr., and C. Cohen (2002), The impact on simulated storm structure and intensity of variations in the mixed layer and moist layer depths, *Mon. Weather Rev.*, 130, 1722–1748, doi:10.1175/1520-0493(2002)130<1722:TIOSSS>2.0.CO;2.
- Murakami, M. (1983), Analysis of the deep convective activity over the western Pacific and southeast Asia. Part I: Diurnal variation, *J. Meteorol. Soc. Jpn.*, 61, 60–76.
- Nesbitt, S. W., and E. J. Zipser (2003), The diurnal cycle of rainfall and convective intensity according to three years of TRMM measurements, *J. Clim.*, 16, 1456–1475.
- Ohsawa, T., H. Ueda, T. Hayashi, A. Watanabe, and J. Matsumoto (2001), Diurnal variations of convective activity and rainfall in tropical Asia, *J. Meteorol. Soc. Jpn.*, 79, 333–352, doi:10.2151/jmsj.79.333.
- Rafiuddin, M., H. Uyeda, and M. N. Islam (2009), Characteristics of monsoon precipitation systems in and around Bangladesh (online), *Int. J. Climatol.*, doi:10.1002/joc.1949.
- Rajeevan, M., S. Gadgil, and J. Bhate (2008), Active and break spells of the Indian summer monsoon, *Natl. Climate Cent. Res. Rep.* 7, Indian Meteorol. Dept., Pune.
- Ramamurthy, K. (1969), Monsoon of India: Some aspects of the “break” in the Indian southwest monsoon during July and August, in *Forecasting Manual*, 1–57 No. IV 18.3, Indian Meteorol. Dept., Poona, India.
- Rao, K. G. (1986), Sensible heat fluxes during the active and break phases of the southwest monsoon over the Indian region, *Boundary Layer Meteorol.*, 36, 283–294, doi:10.1007/BF00118665.
- Rao, T. N., K. N. Uma, T. M. Satyanarayana, and D. N. Rao (2009), Differences in draft core statistics from wet spell to dry spell over Gadanki (13.5N, 79.2E), India, *Mon. Weather Rev.*, doi:10.1175/2009MWR3057.1.
- Schumacher, C., and R. A. Hauxe Jr. (2003), Stratiform rain in the tropics as seen by the TRMM precipitation radar, *J. Clim.*, 16, 1739–1756, doi:10.1175/1520-0442(2003)016<1739:SRITTA>2.0.CO;2.
- Segal, M., R. W. Arritt, C. Clark, R. Rabin, and J. Brown (1995), Scaling evaluation of the effect of surface characteristics on potential for deep convection over uniform terrain, *Mon. Weather Rev.*, 123, 383–400, doi:10.1175/1520-0493(1995)123<0383:SEOTEO>2.0.CO;2.
- Shinoda, T., and H. Uyeda (2002), Effective factors in the development of deep convective clouds over the wet region of eastern China during the summer monsoon season, *J. Meteorol. Soc. Jpn.*, 80, 1395–1414, doi:10.2151/jmsj.80.1395.
- Short, A. D., and K. Nakamura (2000), TRMM radar observations of shallow precipitation over the tropical oceans, *J. Clim.*, 13, 4107–4124, doi:10.1175/1520-0442(2000)013<4107:TROOSP>2.0.CO;2.
- Shusse, Y., and K. Tsuboki (2006), Dimension characteristics and precipitation efficiency of cumulonimbus clouds in the region far south from the mei-yu front over the eastern Asian continent, *Mon. Weather Rev.*, 134, 1942–1953, doi:10.1175/MWR3159.1.
- Simpson, J., R. F. Adler, and G. R. North (1988), A proposed tropical rainfall measuring mission (TRMM) satellite, *Bull. Am. Meteorol. Soc.*, 69, 278–295, doi:10.1175/1520-0477(1988)069<0278:APTRMM>2.0.CO;2.
- Singh, P., and K. Nakamura (2009), Diurnal variation in summer precipitation over the central Tibetan Plateau, *J. Geophys. Res.*, 114, D20107, doi:10.1029/2009JD011788.
- Takayabu, N. Y. (2006), Rain-yield per flash calculated from TRMM PR and LIS data and its relationship to the contribution of tall convective rain, *Geophys. Res. Lett.*, 33, L18705, doi:10.1029/2006GL027531.
- Wang, B., P. J. Webster, and H. Teng (2005), Antecedents and self-induction of active-break south Asian monsoon unraveled by satellites, *Geophys. Res. Lett.*, 32, L04704, doi:10.1029/2004GL020996.
- Weisman, M. L., and J. B. Klemp (1982), The dependence of numerically simulated convective storms on vertical wind shear and buoyancy, *Mon. Weather Rev.*, 110, 504–520, doi:10.1175/1520-0493(1982)110<0504:TDONSC>2.0.CO;2.
- Williams, E. R., S. A. Rutledge, S. G. Geotis, N. Renno, E. Rasmussen, and T. Rickenbach (1992), A radar and electrical study of tropical “hot towers,” *J. Atmos. Sci.* 49, 1386–1396, doi:10.1175/1520-0469(1992)049<1386:ARAESO>2.0.CO;2.
- Yamada, H. (2008), Numerical simulations of the role of land surface conditions in the evolution and structure of summertime thunderstorms over a flat highland, *Mon. Weather Rev.*, 136, 173–188, doi:10.1175/2007MWR2053.1.
- Yanai, M., and C. F. Li (1994), Mechanism of heating and the boundary-layer over the Tibetan Plateau, *Mon. Weather Rev.*, 122, 305–323, doi:10.1175/1520-0493(1994)122<0305:MOHATB>2.0.CO;2.
- Yasunari, T. (1990), Impact of Indian monsoon on the coupled atmosphere/ocean system in the tropical Pacific, *J. Meteorol. Soc. Jpn.*, 72, 1331–1338.
- Yu, R., T. Zhou, A. Xiong, Y. Zhu, and J. Li (2007), Diurnal variations of summer rainfall over contiguous China, *Geophys. Res. Lett.*, 34, L01704, doi:10.1029/2006GL028129.
- Zipser, E. J. (1994), Deep cumulonimbus cloud system in the tropics with and without lightning, *Mon. Weather Rev.*, 122, 1837–1851, doi:10.1175/1520-0493(1994)122<1837:DCCSIT>2.0.CO;2.

K. Nakamura and P. Singh, Hydrospheric Atmospheric Research Center, Nagoya University, Furocho, Chikusa-ku, Nagoya 464-8601, Japan. (prasamsasingh@gmail.com)